

St. Cloud State University

The Repository at St. Cloud State

Chemistry Faculty Publications

Department of Chemistry

5-2022

Synthesis of a Novel RAS Farnesyl Protein Transferase Inhibitor

Mark F. Mechelke

St. Cloud State University

Anna Mikolchak

St. Cloud State University

Follow this and additional works at: https://repository.stcloudstate.edu/chem_facpubs

 Part of the [Medicinal-Pharmaceutical Chemistry Commons](#)

Recommended Citation

Mechelke, Mark F. and Mikolchak, Anna, "Synthesis of a Novel RAS Farnesyl Protein Transferase Inhibitor" (2022). *Chemistry Faculty Publications*. 11.

https://repository.stcloudstate.edu/chem_facpubs/11

This Article is brought to you for free and open access by the Department of Chemistry at The Repository at St. Cloud State. It has been accepted for inclusion in Chemistry Faculty Publications by an authorized administrator of The Repository at St. Cloud State. For more information, please contact tdsteman@stcloudstate.edu.

SYNTHESIS OF A NOVEL RAS FARNESYL PROTEIN TRANSFERASE INHIBITOR

M.F. Mechelke[†] and A. Mikolchak^{*}

Department of Chemistry and Biochemistry, St. Cloud State University, St. Cloud, MN 56301

Abstract

Mutant RAS proteins are associated with 30% of all human cancers. Unregulated cell growth caused by mutant RAS proteins can be prevented by RAS farnesyl protein transferase (FPTase) inhibitors. A novel FPTase inhibitor has been synthesized incorporating a modified farnesyl “tail” and a customized diphosphate “head”. It is anticipated that the modified “tail”, incorporating a phenyl substituent, will bind more tightly to FPTase due to nonbonding interactions between the aromatic ring and ten aromatic amino acid residues that line the enzyme active site. The altered polar “head”, designed from L-aspartic acid, has already been shown to mimic the natural substrate’s diphosphate moiety. It is anticipated that the bioactivity of the novel compound presented in this research will illustrate the relevance of modifications to the farnesyl “tail” in the design of farnesyl diphosphate mimetics.

[†]corresponding author: mfmechelke@stcloudstate.edu

Keywords: Cancer, RAS Proteins, Farnesyl Protein Transferase, Farnesyl Diphosphate, Competitive Inhibitors, Aspartic Acid, Farnesyl Analogues

Introduction

Mammalian *ras* genes encode for RAS proteins that play an essential role in the signal transduction pathways which regulate cell proliferation.¹ Initially synthesized as cytosolic precursors, RAS proteins must first become membrane-bound in order to demonstrate their signaling activity. To associate with the plasma membrane, RAS proteins must undergo a series of post-translational modifications. The first step in modification of the cytosolic RAS precursor is farnesylation of a cysteine amino acid residue located near the RAS carboxy-terminus (Figure 1).² Farnesyl protein transferase (FPTase) is the enzyme that catalyzes this transfer of a farnesyl group to the cysteine residue.³ Modified in this manner, RAS proteins become sufficiently hydrophobic to associate with the plasma membrane.

Once bound to the plasma membrane, RAS proteins act as a molecular switch for cell growth by binding to guanosine diphosphate (GDP) or guanosine triphosphate (GTP).⁴ When RAS is bound to GDP, the switch is “off” - no signaling activity is observed. On the other hand, when RAS is bound to GTP, the switch is “on” - signals for cell proliferation are delivered to the cell nucleus. In this way, RAS proteins play a critical role in the control of normal and transformed cell growth.

The association between RAS and cancer arises from the fact that 30% of all human malignancies contain *ras* genes which encode for RAS proteins that are mutated.¹ These mutant RAS proteins are unable to catalyze the hydrolysis of GTP to GDP. This leads to a broken switch. The switch can be turned “on” - signaling for cell growth, but once “on” it cannot be turned “off”. The build-up of RAS-GTP complexes leads to excessive “on” signal-

ing activity which in the simplest sense is the definition of cancer.

The RAS farnesylation process is an attractive target to prevent unregulated cell growth. Post-translational farnesylation has been proven to be the key step in RAS localization to the plasma membrane and subsequent signaling activity. RAS proteins that cannot be farnesylated do not induce malignant transformations.⁵ Development of methods to decrease RAS farnesylation may lead to new anti-cancer drugs.

One approach to inhibit RAS farnesylation is to design farnesyl diphosphate mimetics. Farnesyl diphosphate can be viewed as a composite of two structural units, the hydrophobic farnesyl “tail” and the highly charged diphosphate “head”. A plethora of research has been published on the design and biological evaluation of novel farnesyl “heads” that have been attached to farnesyl “tails” to prepare competitive inhibitors of FPTase.⁶⁻¹⁰ The difference between these compounds and the natural substrate, farnesyl diphosphate, is that the modified polar “head” is not a good leaving group. These compounds work by outcompeting farnesyl diphosphate for the enzyme active site, thus preventing RAS farnesylation.

The research in this paper illustrates the placement of a previously reported diphosphate “head” mimetic, an L-aspartic acid analogue, onto a modified farnesyl “tail”.⁹ The “tail” that has been prepared contains a phenyl ring (Figure 2). Synthetic routes to this “tail” have been previously investigated.¹¹ It is hypothesized that this aromatic ring will increase binding of the farnesyl diphosphate mimetic to the FPTase enzyme active site. The active site has been shown to contain an α - α barrel that is lined with ten aromatic amino acid residues.¹² Placing a phenyl ring in the “tail” is anticipated to increase binding affinity due to nonbonding interactions, pi stacking, between the phenyl ring and the aromatic amino acids surrounding the cleft.

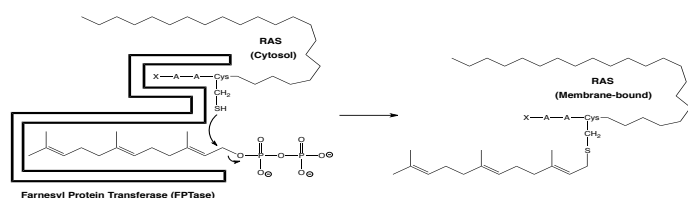


Figure 1. RAS Farnesylation

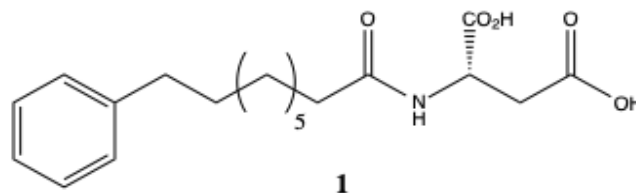


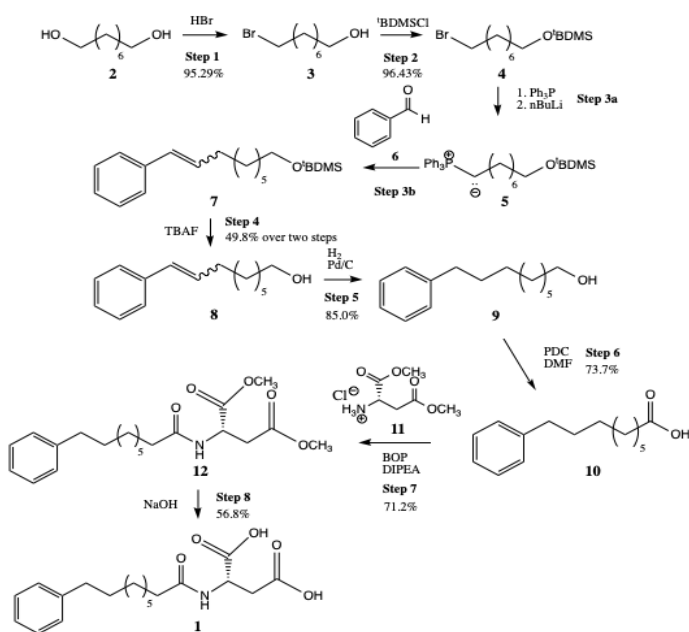
Figure 2. Targeted Farnesyl Diphosphate Mimetic

Past research has illustrated that this hypothesis has merit. Dr. Mark Distefano prepared FPTase inhibitors with benzoylbenzyl groups in the “tail”.¹³ These compounds were developed to gain information about the interactions between proteins and prenyl pyrophosphates through photoaffinity labeling studies. Dr. Distefano discovered that the presence of the benzoylbenzyl group in the “tail” resulted in an approximately 1.5-fold increase in binding affinity to FPTase as compared to the natural substrate. These findings support the hypothesis that aromatic rings in the “tail” will increase FPTase inhibitory activity.

Experimental Methods

Column chromatography was performed using 230-400 mesh silica gel. NMR was recorded on a JEOL 400 MHz NMR spectrometer. Gas chromatography-mass spectrometry was carried out on an Agilent Technologies 7890/5975C gas chromatograph-mass spectrometer. The GC column (30 m x 0.25 mm) has a 0.25 mm polydimethylsiloxane (PDMS) with 5% phenyl substitution stationary phase. The oven conditions will be specifically described for each step. All starting materials were purchased from Millipore Sigma and used as received.

Scheme 1. Synthetic Sequence of Novel FPTase Inhibitor 1



Step 1¹¹

Commercially available 1,8-octanediol (**2**) (1.456 g, 9.957 mmol) was placed into a 100 mL round bottom flask containing a magnetic stir bar and dissolved in toluene solvent (25 mL). Hydrobromic acid (48 wt% in water) (4.50 mL, 39.8 mmol) was added to the flask and the resulting biphasic mixture was heated at reflux (125 °C oil bath) for exactly 30 minutes. The reaction mixture was cooled to room temperature, diluted with brine (25 mL), and extracted two times with hexanes (30 mL and 20 mL respectively). The organic layers were combined, dried over magnesium sulfate, filtered, and concentrated. Mono-brominated product **3** was isolated as a yellow oil (1.983 g, 95.29%). The crude product **3** (93.7%

pure) was shown by GC-MS to contain small amounts of 1,8-dibromooctane impurity (4.8%, RT = 4.069 min) and 1,8-octanediol starting material **2** (1.5%, RT = 2.794 min). The crude product **3** was carried directly into step 2 without further purification. ¹H NMR (400 MHz, CDCl₃) δ 3.63 (br s, 1H), 3.41 (t, *J* = 6.8 Hz, 2H), 3.24 (t, *J* = 6.8 Hz, 2H), 1.69 (tt, *J* = 6.8, 6.8 Hz, 2H), 1.43-1.33 (m, 2H), 1.32-1.22 (m, 2H), 1.22-1.12 (m, 6H). ¹³C NMR (100 MHz, CDCl₃) δ 62.3, 34.0, 32.8, 32.6, 29.3, 28.8, 28.1, 25.7. GC-MS¹⁴ RT = 3.434 min, (*M*⁺-46) = 162, 164 (loss of water and ethylene).

Step 2¹¹

Crude product **3** (1.941 g, 9.282 mmol) was dissolved in dichloromethane (25 mL) and subsequently treated with *tert*-butyldimethylsilyl chloride (1.544 g, 10.24 mmol) and imidazole (0.761 g, 11.2 mmol). The reaction mixture was allowed to stir for one hour at room temperature. The resulting mixture was quenched with brine (40 mL) and extracted twice with diethyl ether (2 x 50 mL). The combined organic layers were dried over magnesium sulfate, filtered, and concentrated to provide silyl ether **4** as a clear oil (2.891 g, 96.43%). The crude product **4** (89.7% pure) was shown by GC-MS to contain small amounts of di-silyl protected impurity (7.5%, RT = 6.739 min) and di-brominated impurity (2.8%, RT = 4.069 min). The crude silyl ether **4** was carried directly into step 3 without further purification. ¹H NMR (400 MHz, CDCl₃) δ 3.58 (t, *J* = 6.8 Hz, 2H), 3.38 (t, *J* = 6.8 Hz, 2H), 1.83 (tt, *J* = 7.0, 7.0 Hz, 2H), 1.53-1.35 (m, 4H), 1.35-1.24 (m, 6H), 0.87 (s, 9H), 0.02 (s, 6H). ¹³C NMR (100 MHz, CDCl₃) δ 63.3, 34.0, 32.9(2C), 29.3, 28.8, 28.2, 26.1(3C), 25.8, 18.4, -5.2(2C). GC-MS¹⁴ RT = 5.567 min, (*M*⁺-57) = 265, 267 (loss of *tert*-butyl).

Steps 3a and 3b¹¹

Crude silyl ether **4** (2.899 g, 8.975 mmol) was treated with triphenylphosphine (2.590 g, 9.873 mmol) and heated, with a reflux condenser attached, at 125 °C for one hour. The resultant solution was removed from the oil bath and THF (15 mL) was added through the reflux condenser. The THF was added to the hot reaction mixture to prevent the reaction from solidifying. The reaction mixture was then placed in an ice bath and cooled to 0 °C. The reflux condenser was removed and the flask was sealed with a rubber septum. An empty needle was placed through the septum to serve as a vent. *n*BuLi (2.5 M in hexanes, 3.95 mL, 9.87 mmol) was slowly added. The reaction mixture turned a bright orange color; the color represents formation of ylide **5**. The flask was removed from the ice bath and the colored solution was allowed to stir for 15 minutes as it warmed to room temperature. Benzaldehyde (**6**) (0.91 mL, 9.0 mmol) was added to ylide **5** and the reaction was stirred for an additional 20 minutes. The solution turned a cloudy yellow color. 1.0 M HCl (aq) was added to the reaction mixture until a pH of 4 was achieved (approximately 6.0 mL). The reaction mixture was diluted with distilled water and extracted twice with diethyl ether (50 mL and 30 mL respectively). The organic layers were combined, dried over magnesium sulfate, filtered, and concentrated. Crude product **7** was spotted on a thin layer chromatography (TLC) plate against benzaldehyde (**6**) using 20% ethyl acetate in hexanes as the elution solvent. The TLC plate was visualized with short wave UV light and stained with potassium permanganate. The desired Wittig reaction *cis/trans* product **7** had an *R*_f value of 0.72. A small spot at *R*_f = 0.20 was later identified as deprotected alcohol **8**. Other spots observed on the plate were triphenylphosphine and triphenylphosphine oxide. GC-MS¹⁵

analysis of crude product **7** illustrated the following major compounds: RT = 8.630 min triphenylphosphine oxide (27.4%); RT = 6.123 min product **7** (*trans*) (28.4%); RT = 5.730 min triphenylphosphine; RT = 5.688 min product **7** (*cis*) (39.7% with triphenylphosphine; could not integrate separately). The crude product was carried directly into step 4. The *trans* and *cis* product **7** assignments were later confirmed using ¹H NMR and GC-MS analysis of the purified step 4 product.

Step 4¹¹

The crude step 3 product (assumed a theoretical yield of product **7**, 8.975 mmol) was treated with tetrabutylammonium fluoride (TBAF) (1.0 M in THF, 18.0 mL, 18.0 mmol). No additional solvent was added. The reaction was allowed to stir for one hour at room temperature. The resulting solution was diluted with saturated ammonium chloride (aqueous) (25 mL) and extracted with diethyl ether (2 x 50 mL). The combined organic layers were dried over magnesium sulfate, filtered, and concentrated. The resultant oil was purified by column chromatography (25% ethyl acetate in hexanes) to afford the desired deprotected product **8** (0.974 g, 49.8% yield over the two steps – steps 3 and 4). The product was a heavy mixture of *trans:cis* isomers (1.1 *trans*: 1.0 *cis*) as illustrated by both GC-MS and ¹H NMR data. ¹H NMR (400 MHz, CDCl₃) δ 7.41-7.28 (m, 4H), 7.27-7.19 (m, 1H), 6.46 (d, *J* = 11.8 Hz, 1H *cis*), 6.42 (d, *J* = 15.8 Hz, 1H *trans*), 6.26 (dt, *J* = 15.8, 6.8 Hz, 1H *trans*)*, 5.70 (dt, *J* = 11.8, 7.2 Hz, 1H *cis*)*, 4.11 (br s, 1H), 3.65 (t, *J* = 6.8 Hz, 2H *cis/trans*), 3.63 (t, *J* = 6.8 Hz, 2H *cis/trans*), 2.38 (dtd, *J* = 7.6, 7.6, 1.6 Hz, 2H *cis*)*, 2.24 (dtd, *J* = 7.6, 7.6, 1.0 Hz, 2H *trans*)*, 1.65-1.55 (m, 2H), 1.55-1.45 (m, 2H), 1.44-1.31 (m, 6H). GC-MS¹⁵ RT = 4.613 min, M⁺ = 218 (*trans*); RT = 4.303 min, M⁺ = 218 (*cis*)**

*The ratio of *trans:cis* stereoisomers was determined from ¹H NMR to be 1.13 *trans* : 1.00 *cis*.

**The ratio of *trans:cis* stereoisomers was determined from GC to be 1.15 *trans*: 1.00 *cis*.

Step 5¹¹

Trans and *cis* alkenes **8** (0.919 g, 4.22 mmol) were dissolved in methanol (10.0 mL) and treated with 10% palladium/charcoal (by weight) (0.508 g, 0.477 mmol). A hydrogen balloon was inserted into the flask and the flask was purged of air through a vented septum. The hydrogen balloon was refilled and the flask was allowed to stir for 20 hours. The resulting palladium/charcoal slurry was filtered through a thin layer of silica gel over Celite. The filtration funnel was rinsed thoroughly with ethyl acetate (approximately 75 mL). Concentration of the filtrate provided alcohol **9** (0.789 g, 85.0%). Characterization of the product by GC-MS and NMR showed that no further purification was necessary. ¹H NMR (400 MHz, CDCl₃) δ 7.32 (dd, *J* = 6.8, 6.8 Hz, 2H), 7.25-7.18 (m, 1H), 7.22 (d, *J* = 7.2 Hz, 2H), 4.00 (br s, 1H), 3.65 (t, *J* = 6.8 Hz, 2H), 2.65 (t, *J* = 7.6 Hz, 2H), 1.72-1.56 (m, 4H), 1.43-1.32 (m, 10H). ¹³C NMR (100 MHz, CDCl₃) δ 143.0, 128.5(2C), 128.4(2C), 125.7, 62.8, 36.2, 32.8, 31.7, 29.8, 29.7(2C), 29.5, 26.0. GC-MS¹⁵ RT = 4.316 min, M⁺ = 220.

Step 6¹⁶

9-phenyl-1-nonanol (**9**) (0.787 g, 3.58 mmol) was dissolved in dimethylformamide (DMF) (30 mL) and treated with pyridinium dichromate (PDC) (8.07 g, 21.5 mmol). The reaction mixture was

allowed to stir at room temperature for 20 hours. The mixture was diluted with water (25 mL) and extracted with ethyl acetate (50 mL). The organic layer was washed with brine (2 x 20 mL), dried over magnesium sulfate, filtered, and concentrated. The isolated carboxylic acid **10** (0.617 g, 73.7%) was shown to be very pure by GC-MS and NMR analysis. ¹H NMR (400 MHz, CDCl₃) δ 10.70 (br s, 1H), 7.30 (dd, *J* = 7.2, 7.2 Hz, 2H), 7.23-7.17 (m, 1H), 7.20 (d, *J* = 7.2 Hz, 2H), 2.63 (t, *J* = 7.6 Hz, 2H), 2.37 (t, *J* = 7.2 Hz, 2H), 1.71-1.60 (m, 4H), 1.41-1.29 (m, 8H). ¹³C NMR (100 MHz, CDCl₃) δ 180.2, 143.0, 128.5(2C), 128.4(2C), 125.7, 36.1, 34.3, 31.6, 29.6, 29.4, 29.3, 29.2, 24.8. GC-MS¹⁵ RT = 4.618 min, M⁺ = 234.

Step 7⁹

9-phenylnonanoic acid (**10**) (0.617 g, 2.64 mmol) was dissolved in acetonitrile (13.0 mL) and DMF (4.6 mL). Commercially available L-Aspartic acid methyl ester (**11**) (0.531 g, 2.69 mmol) was added. The reaction was subsequently treated with benzotriazole-1-yloxytris(dimethylamino)phosphonium hexafluorophosphate (BOP) reagent (1.20 g, 2.71 mmol) followed by diisopropylethylamine (1.38 mL, 7.92 mmol). The reaction was placed under nitrogen gas and allowed to stir for 16 hours at room temperature. The solution turned an orange color. The reaction was quenched with 1.0 M HCl (aqueous) (50 mL) and extracted with ethyl acetate (2 x 50 mL). The combined organic layers were washed sequentially with 10% sodium carbonate (aqueous) (50 mL) and 10% lithium chloride (aqueous) (2 x 50 mL). The organic layer was dried over magnesium sulfate, filtered, and concentrated to afford crude diester **12**. The crude product was purified by column chromatography (10% hexanes in ethyl acetate) to afford pure diester **12** (0.709 g, 71.2%). ¹H NMR (400 MHz, CDCl₃) δ 7.19 (dd, *J* = 7.2, 7.2 Hz, 2H), 7.12-7.06 (m, 1H), 7.10 (d, *J* = 7.6 Hz, 2H), 6.69 (d, *J* = 7.8 Hz, 1H), 4.82 (ddd, *J* = 7.8, 4.4, 4.4 Hz, 1H), 3.66 (s, 3H), 3.60 (s, 3H), 2.96 (dd, *J* = 17.2, 4.4 Hz, 1H), 2.80 (dd, *J* = 17.2, 4.4 Hz, 1H), 2.52 (t, *J* = 7.6 Hz, 2H), 2.16 (t, *J* = 7.6 Hz, 2H), 1.61-1.48 (m, 4H), 1.30-1.19 (m, 8H). ¹³C NMR (100 MHz, CDCl₃) δ 173.1, 171.6, 171.4, 142.8, 128.4(2C), 128.3 (2C), 125.6, 52.7, 52.0, 48.5, 36.3, 36.2, 36.0, 31.5, 29.4, 29.3, 29.3, 29.2, 25.6. GC-MS¹⁷ RT = 22.781 min, M⁺ = 377.

Step 8⁹

Diester **12** (0.709 g, 1.88 mmol) was dissolved in absolute ethanol (15 mL) and treated with 1.0 M sodium hydroxide (aqueous) (4.00 mL, 4.00 mmol). The resulting yellow solution was allowed to stir at room temperature for four hours. The reaction was concentrated on a rotary evaporator to a yellow, crystalline solid. Distilled water (10 mL) and 1.0 M HCl (aqueous) (10 mL) were added to the flask and the resultant mixture was extracted with dichloromethane (2 x 50 mL). The combined organic layers were dried over magnesium sulfate, filtered, and concentrated to provide diacid **1** (0.373 g, 56.8%) as a white solid. ¹H NMR (400 MHz, DMSO-d₆) δ 12.4 (br s, 2H), 8.06 (d, *J* = 8.0 Hz, 1H), 7.22 (dd, *J* = 7.2, 7.2 Hz, 2H), 7.14 (d, *J* = 6.4 Hz, 2H), 7.11 (t, *J* = 7.6 Hz, 1H), 4.46 (m, 1H), 2.63 (dd, *J* = 16.4, 5.6 Hz, 1H), 2.54-2.45 (m, 3H), 2.03 (t, *J* = 6.8 Hz, 2H), 1.55-1.46 (m, 2H), 1.46-1.38 (m, 2H), 1.28-1.13 (m, 8H). ¹³C NMR (100 MHz, DMSO-d₆) δ 173.1, 172.6, 172.2, 142.9, 128.8(2C), 128.7(2C), 126.1, 49.0, 36.6, 35.7, 35.5, 31.6, 29.3(2C), 29.2, 29.0, 25.7. GC-MS¹⁷ RT = 24.539 min, (M⁺-18) = 331 (loss of water).

Results and Discussion

The synthesis of novel FPTase inhibitor **1** started with the mono-bromination of commercially available 1,8-octanediol (**2**) (Scheme 1).¹¹ The only difficulty in this step was yield optimization. If the reaction was heated at reflux for too short of a time frame, poor conversion of diol **2** to mono-bromide **3** was observed. If the reaction was heated for too long, mono-bromide **3** continued to react and made the undesired di-bromide product, 1,8-dibromooctane. It was discovered that heating the reaction for exactly 30 minutes provided the optimal yield of mono-brominated product **3**. The ratio of products was determined by gas chromatography (GC) to be 62.5: 3.2: 1.0 mono-brominated product **3**: di-brominated product: 1,8-octanediol (**2**). This crude product was carried directly into the second step.

In the second step of the sequence, the alcohol functional group in mono-bromide **3** was protected with a *tert*-butyldimethylsilyl ether. The resultant silyl ether **4** was isolated in high yield with the expected minor di-brominated and di-silylated impurities also visible on the GC trace. The ratio of products carried into step 3 was 32.0: 2.7: 1.0 silyl ether **4**: di-silylated 1,8-octanediol: 1,8-dibromooctane.

Silyl ether **4** was carried directly into the Wittig reaction, step 3. Addition of triphenylphosphine to silyl ether **4** afforded the phosphonium salt which was subsequently treated with *n*-butyllithium to make phosphorus ylide **5**. Nucleophilic addition of ylide **5** to benzaldehyde (**6**) resulted in formation of alkene **7**.¹¹ GC-MS and thin layer chromatography of crude alkene **7** displayed four major compounds – *trans*-alkene **7**, *cis*-alkene **7**, triphenylphosphine, and triphenylphosphine oxide. A minor product was identified as deprotected alcohol **8**. Further purification was not performed on the step 3 product for two reasons. First, the R_f values of product **7** and the triphenylphosphine impurities were close enough that it made purification by column chromatography difficult. Second, the Wittig reaction conditions caused some of alkene **7** to be deprotected to produce alcohol **8**. Since removal of the silyl protecting group was the next step in the synthetic sequence and the more polar alcohol **8** was much easier to separate from the triphenylphosphine impurities, crude product **7** was carried directly into step 4. Unfortunately, at this time the ratio of *trans* to *cis* alkene **7** isomers could not be calculated because the *cis* isomer peak overlapped with the triphenylphosphine peak on the GC trace (retention times of 5.688 and 5.730 minutes respectively).

In the initial attempt to deprotect silyl ether **7**, 1.1 equivalents of tetrabutylammonium fluoride (TBAF) were used. After stirring for 30 minutes, only approximately 52% deprotection to alcohol **8** was observed by GC. The best conversion to alcohol **8** was found to require 2.0 equivalents of TBAF and one hour of stirring at room temperature. The crude product was purified by column chromatography to afford a mixture of *trans* and *cis* alcohol **8**. The ratio of *trans*:*cis* isomers was determined to be 1.1:1:0 based on integration of both the GC trace and ¹H NMR spectrum.

In step 5, the heavy mixture of *trans*:*cis* isomers **8** was hydrogenated with hydrogen gas and palladium catalyst. Alcohol **9** was isolated in 85.0% yield and no further purification was required. Oxidation of alcohol **9** to carboxylic acid **10** was performed using

pyridinium dichromate (PDC) with dimethylformamide (DMF) solvent.¹⁶ One of the attractive attributes of this synthetic sequence was the purity of the crude products. Column chromatography only had to be performed after two reactions, steps 4 and 7.

To complete the synthesis of novel FPTase inhibitor **1**, a peptide bond had to be formed between carboxylic acid **10** and L-Aspartic acid methyl ester (**11**). This coupling reaction proceeded very smoothly using the benzotriazole-1-yloxytris(dimethylamino)phosphonium hexafluorophosphate (BOP) reagent.⁹ Purification by column chromatography afforded pure dimethyl ester **12** in 71.2% yield. Diester **12** was then treated with sodium hydroxide in a standard saponification reaction. The only difficulties encountered in this step were in the isolation of diacid **1**. Concentration of the saponification reaction provided the diacid salt. This salt was initially dissolved in water and quenched with 1.0 M HCl until a pH of 5 was achieved. Extraction of the aqueous layer with diethyl ether, however, provided no product in the organic layer as observed by GC-MS analysis. The aqueous layer was then treated with a large excess of 1.0 M HCl and extracted with a more polar solvent, dichloromethane. GC-MS analysis of the dichloromethane layer revealed diacid **1**. The organic layer was then concentrated and diacid **1** was isolated as a white solid.

In conclusion, novel FPTase inhibitor **1** was prepared in 8 steps with an 11.6% overall yield. This correlates to an average yield of 76.4% per step. The entire sequence was performed with only two column chromatography purifications, making this an efficient, cost-effective route to diacid **1**. It is anticipated that diacid **1**, incorporating an aromatic ring in the “tail”, will help to illuminate the importance of nonbonding interactions in the binding of FPTase inhibitors to the enzyme active site.

References

- (1) Barbacid, M. *Ann. Rev. Biochem.*, **1987**, *56*, 779-827.
- (2) Hancock, J.F.; Magee, A.I.; Childs, J.E., Marshall, C.J. *Cell*, **1989**, *57*, 1167-1177.
- (3) Reiss, Y.; Goldstein, J.L.; Seabra, M.C.; Casey, P.J.; Brown, M.S. *Cell*, **1990**, *62*, 81-88.
- (4) Boguski, M.S.; McCormick, F. *Nature*, **1993**, *366*, 643-654.
- (5) Willumsen, B.M.; Norris, K.; Papageorge, A.G.; Hubbert, N.L.; Lowy, D.R. *EMBO J.*, **1984**, *3*, 2581-2585.
- (6) Biller, S.A.; Sofia, M.J.; DeLange, B.; Forster, C.; Gordon, E.M.; Harrity, T.; Rich, L.C.; Ciosek Jr., C.P. *J. Am. Chem. Soc.*, **1991**, *113*, 8522-8524.
- (7) Magnin, D.R.; Biller, S.A.; Dickson Jr., J.K.; Logan, J.V.; Lawrence, R.M.; Chen, Y.; Sulsky, R.B.; Ciosek Jr., C.P.; Harrity, T.W.; Jolibois, K.G.; Kunselman, L.K.; Rich, L.C.; Slusarchyk, D.A. *J. Med. Chem.*, **1995**, *38*, 2596-2605.
- (8) Valnetijn, A.R.P.M.; Van den Berg, O.; Van der Marel, G.A.; Cohen, L.H.; Van Boom, J.H. *Tetrahedron*, **1995**, *51*, 2099-2108.
- (9) Patel, D.V.; Schmidt, R.J.; Biller, S.A.; Gordon, E.M.; Robinson, S.S.; Manne, V. *J. Med. Chem.*, **1995**, *38*, 2906-2921.
- (10) Pompliano, D.L.; Rands, E.; Schaber, M.D.; Mosser, S.D.; Anthony, N.J.; Gibbs, J.B. *Biochemistry*, **1992**, *31*, 3800-3807.
- (11) Mechelke, M.F.; Motschke, L.; Nichols, T.; Albrecht, S. *Journal of Undergraduate Chemistry Research* **2009**, *8*, 43-48.

- (12) Park, H.-W.; Boduluri, S.R.; Moomaw, J.F.; Casey, P.J.; Beese, L.S. *Science*, **1997**, *275*, 1800-1805.
- (13) Gaon, I.; Turek, T.C.; Distefano, M.D. *Tetrahedron Lett.* **1996**, *37*, 8833–8836.
- (14) GC-MS oven conditions for Steps 1 and 2: 150 °C for 2 minutes; Ramp 20 °C/min up to 250 °C; Hold at 250 °C for 1 min
- (15) GC-MS oven conditions for Steps 3 thru 6: 170 °C for 2 minutes; Ramp 40 °C/min up to 250 °C; Hold at 250 °C for 8 min
- (16) Ortar, G.; Cascio, M.G.; De Petrocellis, L.; Morera, E.; Rossi, F.; Schiano-Moriello, A.; Nalli, M.; De Novellis, V.; Woodward, D.F.; Maione, S.; Di Marzo, V. *J. Med. Chem.* **2007**, *50*, 6554-6569.
- (17) GC-MS oven conditions for Steps 7 and 8: 70 °C for 2 minutes; Ramp 20 °C/min up to 250 °C; Hold at 250 °C for 15 min